Carbonate Heterogeneity Based on Lithofacies and Petrography of the Jurassic Twin Creek Limestone in Pineview Field, Northern Utah Thrust Belt

David E. Eby
Eby Petrography & Consulting, Inc.
Denver, Colorado

Thomas C. Chidsey, Jr., and Douglas A. Sprinkel
Utah Geological Survey
Salt Lake City, Utah

Abstract

The Middle Jurassic Twin Creek Limestone in the Utah/Wyoming thrust belt has produced over 15 million BO and 93 BCFG. The Twin Creek was deposited in a shallow-water embayment south of the main body of a Middle Jurassic sea. Traps from on subsidiary closures along major ramp anticlines where the low-porosity Twin Creek is extensively fractured. Hydrocarbons in Twin Creek Limestone reservoirs were generated from subthrust Cretaceous source rocks. Seals, barriers, and baffles for the producing horizons are overlying argillaceous and clastic beds, and non-fractured units within the Twin Creek. Productive members have little to no primary porosity but exhibit secondary porosity in the form of fracturing. Natural and open fractures provide good permeability pathways within these very low porosity rocks.

Analysis of core from Pineview field in the northern Utah part of the thrust belt revealed complex heterogeneity due to a variety of carbonate lithofacies, textures, structures, and diagenesis (fracturing and stylolitization). Lithofacies include open marine, low- to high-energy middle shelf, microbial mats/tidal flat, marine sabkha, inner shelf microbial lagoon, oolitic shoals, and terrestrial siliciclastics. Carbonate fabrics consist of microbially laminated mudstone, wackestone, packstone, grainstone/rudstone, and thrombolite boundstone with beds of siltstone and shale. These units may contain variable amounts of peloids, hypersaline (broken and "cerebroid"), oolites, oncolites, soft pellets, and skeletal grains (including crinoids, bryozoans, brachiopods, benthic forams, and bivalves). Sedimentary structures include mud cracks, ripples, cross-beds, burrows, and anhydrite nodules. Mudstone is the dominant fabric for stylolite and fracture development.

Fractures display a complex history of opening, calcite filling, and dissolution. Representative thin sections show nearly parallel, sub-vertical and sub-horizontal swarms of calcite- or anhydrite-filled microfractures. Visible porosity occurs as isolated dissolution pores and partially open microfractures. Both bed-parallel and bed-normal stylolites are common. Replacement dolomite, microporosity, pyrite replacement, and late calcite along fractures or stylolites are common within productive (perferated) intervals of the Twin Creek Limestone.

Outcrop analogs for Twin Creek reservoirs display closely spaced rhombic and rectilinear fracture patterns developed on bedding planes and within dense, homogeneous non-porous (in terms of primary porosity) limestone beds. Thin-bedded siltstone within various members, also observed in outcrop, creates additional reservoir heterogeneity.

Regional Overview

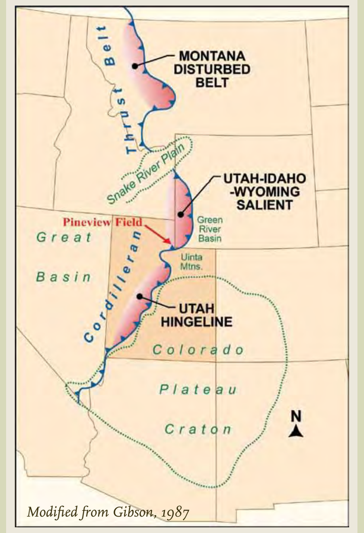

Location of the Cordilleran Thrust Belt including the Montana "Disturbed" Belt, Utah-Idaho-Wyoming Salient, and Utah "Hingeline."

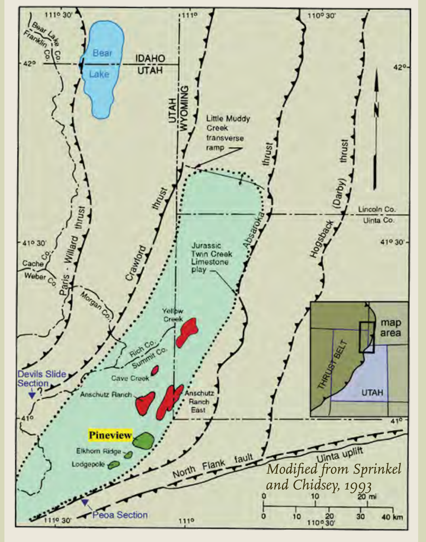

Location of Fields that Produce Oil (green) and Gas and Condensate (red) from the Jurassic Twin Creek Limestone, Utah and Wyoming.

Major thrust faults are dashed where approximate (teeth indicate hanging wall). The Twin Creek Limestone play area (in light green) is shown within the dotted lines. Location of outcrop analogs for this study are also shown.

Age	Formation		Thickness	Lith	Products
K	Kelvin Formation		up to 5700'		
JURASSIC	Stump Formation		60-250		
	Preuss Sandstone		900-1500		salt
	Twin Creek Ls	Giraffe Creek Mbr	110-230		
		Leeds Creek Member	1000-1300		
		Watton Canyon Mbr	400		✱
		Boundary Ridge Mbr	100-250		✱
		Rich Member	420-540		✱
		Sliderock Member	100-230		✱
		Gypsum Spring Mbr	210		✱
					J-1 UNCONFORMITY
	Nugget Sandstone		1100-1500		
Ꝛ	Ankareh Formation	Wood Shale Tongue	520		
		Higham Grit & Timothy SS Mbr	40-200		
		Lanes Shale Tongue	470-700		

Modified from Hintze and Kowallis, 2009

✱ Oil and gas production

Stratigraphic Column of the Jurassic and Bounding Strata, Weber Canyon, Devils Slide Area, Morgan and Summit Counties, Utah .

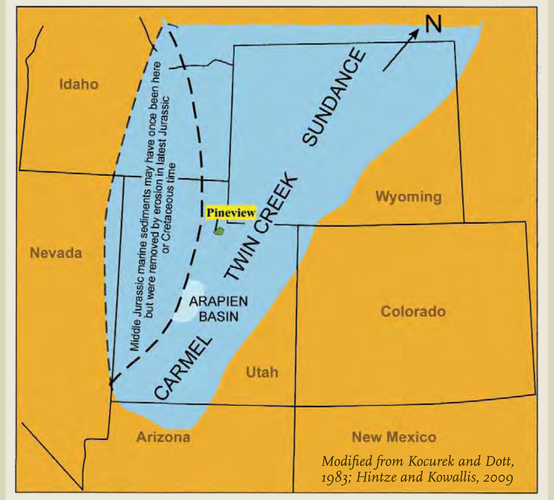

Generalized Map of the Extent of the Middle Jurassic Marine Invasion of the Sundance-Twin Creek-Arapien-Carmel Seas.

Pineview Field General Overview

Twin Creek Limestone Discovery Well

- American Quasar Petroleum Union Pacific No. 3-1 (NWNW Sec. 3, T. 2 N., R. 7 E., Summit Co., Utah)
- T.D. – 10,312 ft (-3125 m)
- Completed – September 1, 1975
- Producing Reservoirs – Jurassic Twin Creek Limestone and Navajo Sandstone
- IPF – 576 BOPD, 420 MCFGPD

Production & Reserves

- Current Operator – Citation Oil & Gas Corp.
- Currently Producing Wells – 4
- Abandoned Producers – 15
- Monthly Production (November 2009) – 5936 BO & 15,230 MCFG
- Cumulative Production (as of December 1, 2009) – 9,126,274 BO & 11.4 BCFG
- Estimated Ultimate Recovery – 12 million BO; 27.3 BCFG
- Secondary Recovery Project – a horizontal drilling program in 1997 consisted of two wells targeting the Watton Canyon Member. Both horizontal lengths were nearly 3000 feet in a north-northeast direction.

Reservoir Data

- Productive Area – 2080 acres
- Spacing – 80 acres
- Gross Pay – 830 ft
- Net Pay – 200 ft
- Net to Gross – 0.24
- Hydrocarbon Column – 1100 ft
- Average Porosity – 2 to 4%
- Permeability – 4 to 30 mD
- Water Saturation – 15 to 35%
- Water Resistivity – 0.160 ohm-m @ 68°F, 25,000 TDS
- BHT – 210°F
- Type of Drive – solution gas drive
- Initial Reservoir Pressure – 4200 psi
- Present Reservoir Pressure – 1000 psi (estimated)

Oil & Gas Characteristics

- API Gravity – 24.1° to 45.7°
- Oil Color – amber to dark brown
- Viscosity – 2.0 cst @ 104°F
- Pour Point – 20° to 70°
- Sulfur, wt% – 0.07%
- Nitrogen, wt% – 0.008%
- GOR – 1000 ft³/bbl
- Associated Gas Composition – 17% methane, 27% ethane, 35% propane, 16% butane, 4% pentane, and 1% other components
- Heating Value – 2321 Btu/ft³

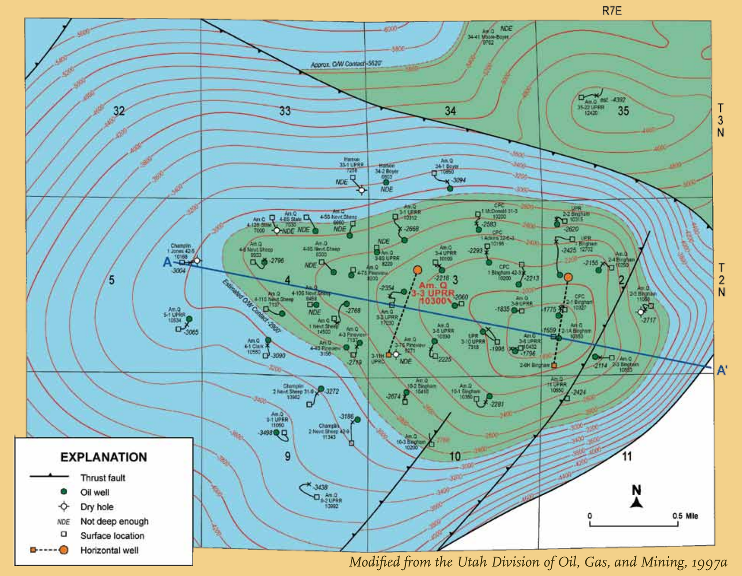

Structure Contour Map of the Top of Watton Canyon Member and Horizontal Wells, Pineview Field

Contour interval = 200 feet, datum = mean sea level. Cross section A–A' shown below.

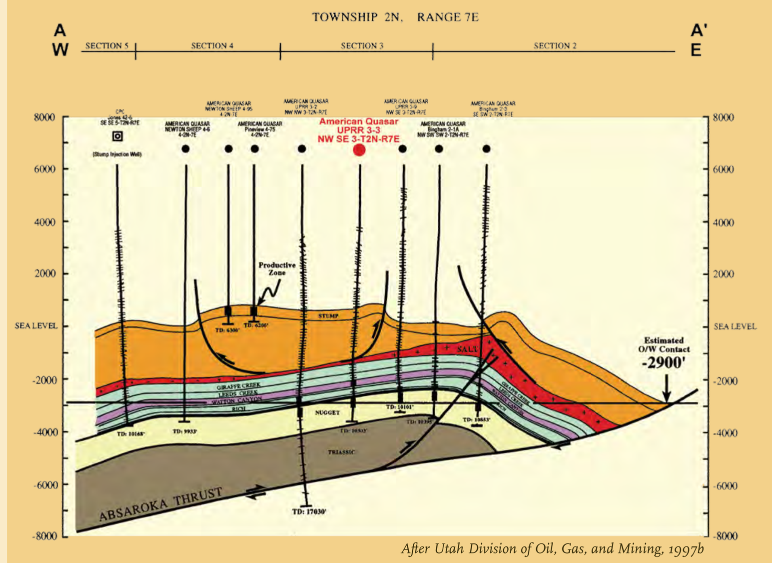

East-West Structural Cross Section, Pineview Field

The Watton Canyon Member of the Twin Creek Limestone, and primary target for horizontal drilling, shown in purple. Dipmeter projections shown on some wellbores.

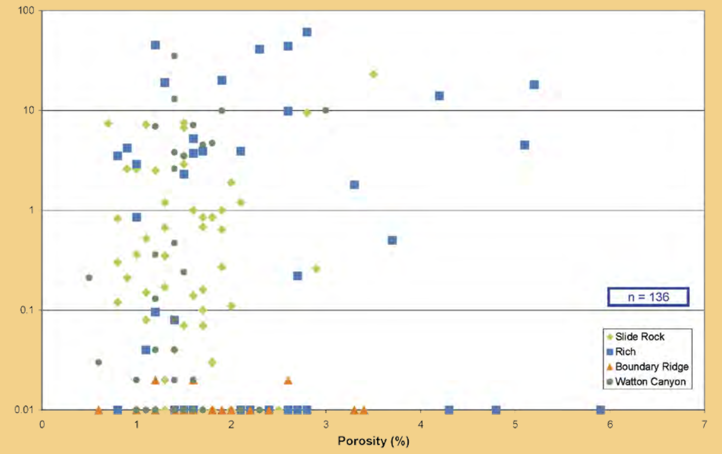

Twin Creek Limestone Porosity/Permeability Cross Plot, UPRR No. 3-3 Well, Pineview Field, Summit County, Utah

Cored Well

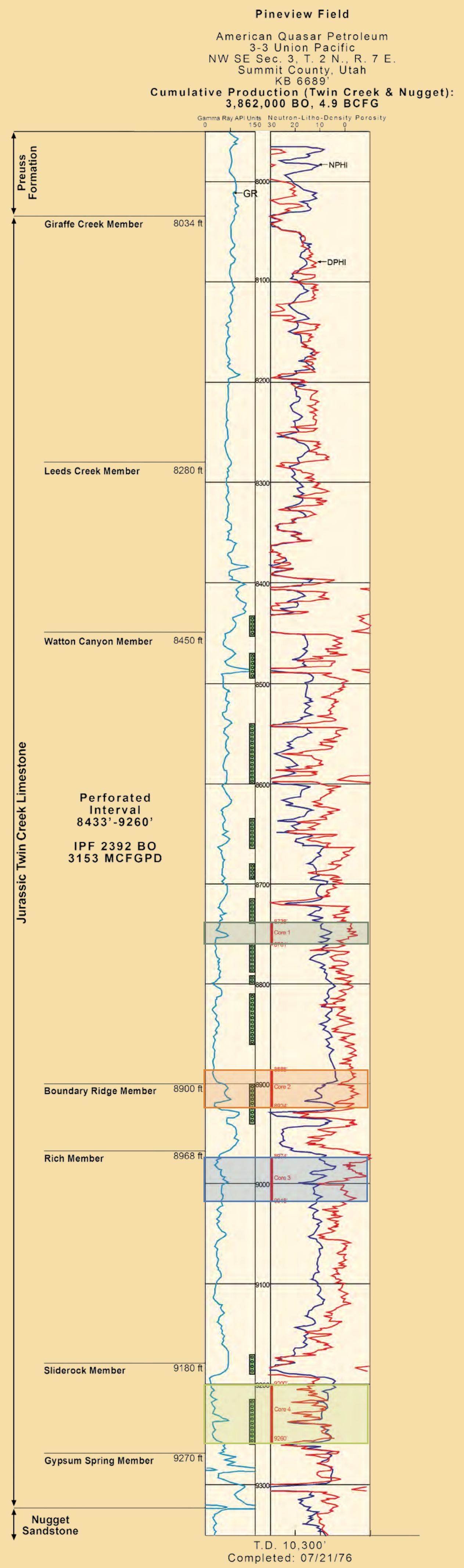

Geophysical Well Log of the Twin Creek Limestone, UPRR No. 3-3 Well, Pineview Field, Summit County, Utah

Lithofacies and Petrography

Panel I

Watton Canyon Member

Core Description

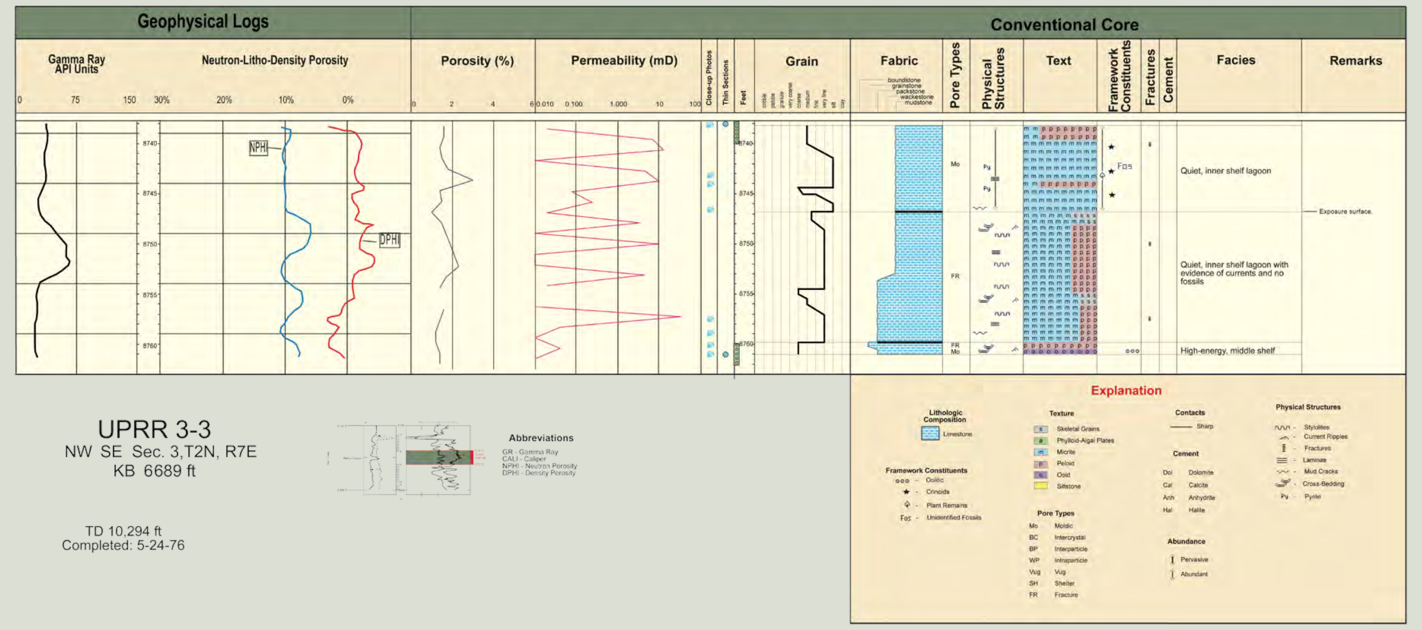

Slabbed core end showing a peloidal packstone incised by a small channel filling containing microbial rip-up clasts (in light gray). See photomicrographs from this core interval. (8738 ft., porosity = 1.6%, permeability = 0.02 mD).

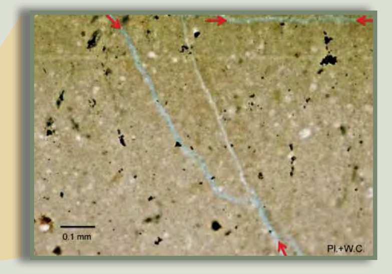

Silty peloidal mudstone with open microfractures (in blue between the red arrows). The black specks are sulfide minerals.

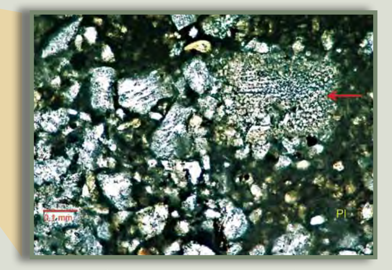

Silt- and fine sand-sized carbonate and siliciclastic grains surrounded by dense lime mud. The red arrow points to an echinoderm grain.

Core through the mid-Watton Canyon Member: 8738 – 8763 ft.

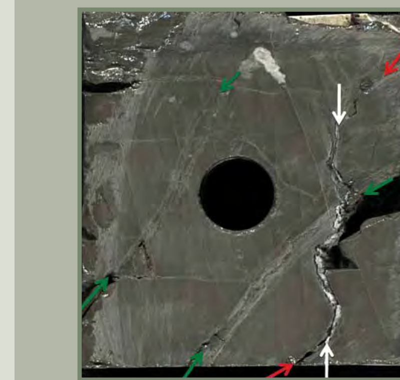

Massive crinoid-bearing lime wackestone to mudstone cut by a bed-normal stylolite (between red arrows), a vertical mineralized fracture (in white, between the white arrows), and oblique open fractures (between the green arrows). (8743 ft., porosity = 3.0%, permeability = 10 mD).

Mineralized surface of a subvertical fracture through a massive lime mudstone. Note the white crystals that prop fractures open. Oil staining and drilling mud impart the brownish color on the mineralized surface. (8744 ft., porosity = 1.4%, permeability = 0.08 mD).

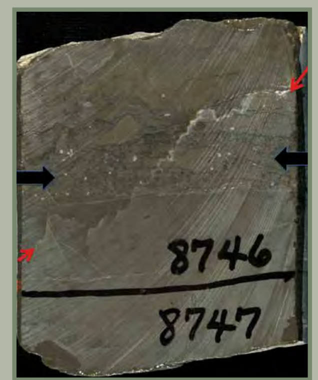

Exposure surface marked by lime mud rip-up clasts (between black arrows) derived from desiccation cracked surfaces. Note the mineralized oblique "stylo-fractures" (between the red arrows). (8747 ft., porosity = 1.5%, permeability = 3.5 mD).

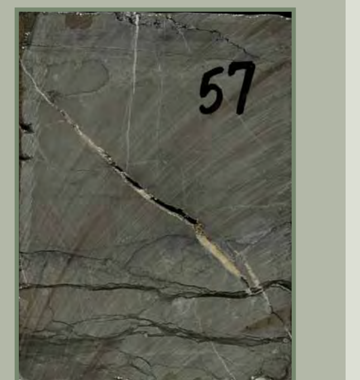

Massive lime mudstone with clusters of wispy seam stylolites and healed vertical fractures. Note the oblique propped open fracture that may be important for high oil production rates. (8757.5 ft., porosity = 1.2%, permeability = 0.04 mD).

Porosity/Permeability Cross Plot

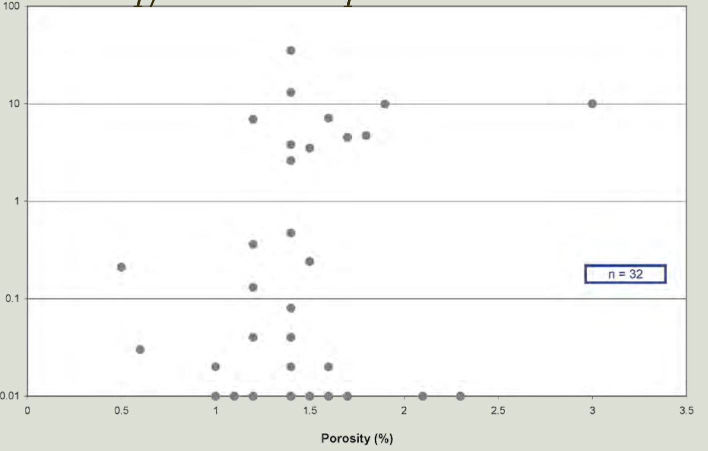

Lime mudstone with mm-scale microbial laminations. Note the vertical (bed normal) stylolites and the healed fractures. (8759 ft., porosity = 1.4%, permeability = 0.01 mD).

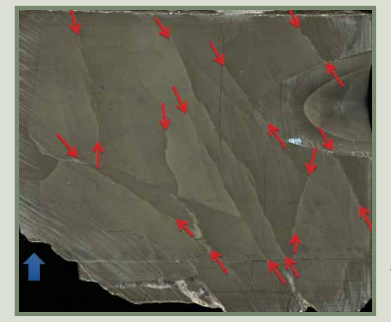

Core closeup: Oblique open fractures that form conjugate sets (between red arrows) within a lime mudstone exhibiting microbial laminations. Fractures with other orientations are mineralized and healed with calcite. (8760 ft., porosity = 1.4%, permeability = 0.01 mD).

Thin bed of ooids (between red arrows) within a massive lime mudstone exhibiting microbial laminae. Note the vertical fractures healed with white calcite. (8761 ft.).

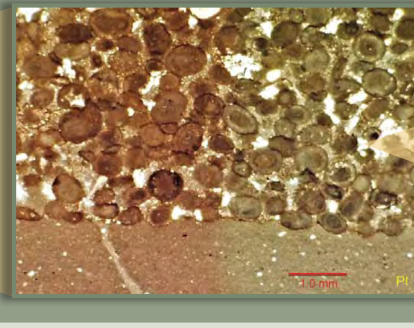

Contact between an oolitic grainstone bed and lime mudstone. Note the rounded quartz silt grains (in white).

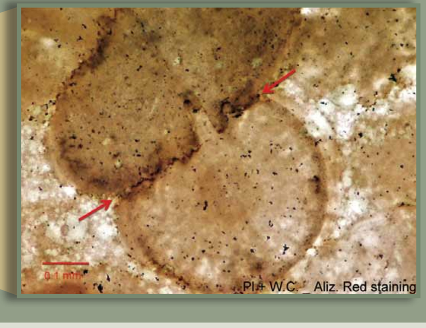

Closeup of a stylolitc contact between ooids (see red arrows), a common post-burial feature of this oolitic grainstone. Note the minor amount of dolomite replacement (in white).

Lithofacies and Petrography

Lower Watton Canyon Member

Nodular lime mudstone with lenses of fossiliferous wackestone. Note the vertical (bed-normal) stylolites and vertical tensional fractures filled with white calcite. (8891.5 ft., porosity = 1.1%, permeability = 0.01 mD).

Fossiliferous wackestone with swarms of mineralized vertical microfractures that are subparallel to the vertical (bed normal) stylolites. The black arrow indicates UP.

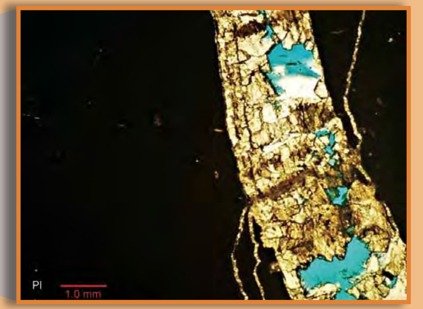

Wide aperture fracture that shows incomplete filling with calcite. Open space within this fracture segment is shown in blue.

Lime mudstone with possible vague microbial laminations. Note the vertical (bed-normal) stylolites (see red arrows). Tension gashes and other fractures are largely filled with white calcite. (8895.5 ft., porosity = 0.5%, permeability = 0.21 mD).

Upper Boundary Ridge Member

Core Description

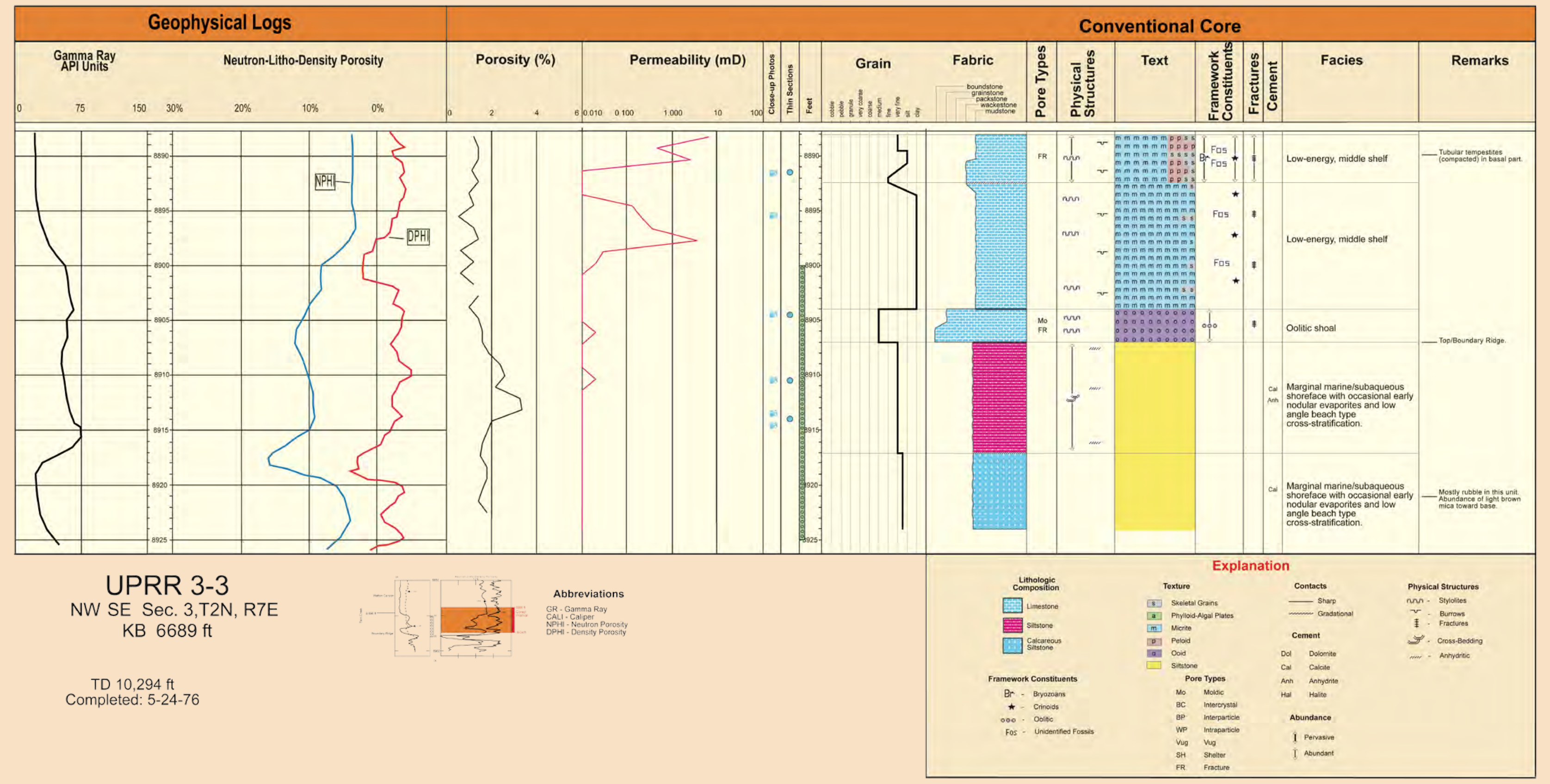

Core composite from 8888-8924 ft., covering the lower Watton Canyon Member and the upper Boundary Ridge Member.

Porosity/Permeability Cross Plot

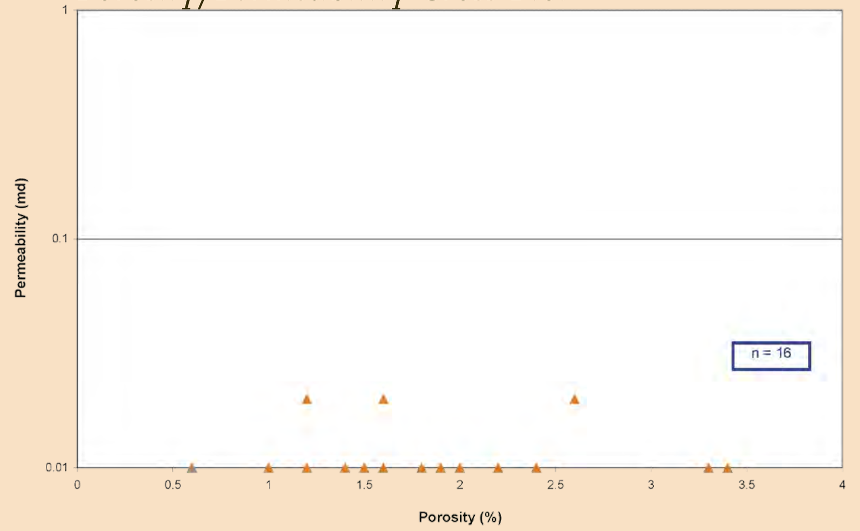

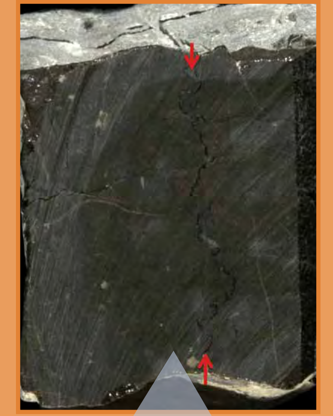

Oolitic and oncolitic grainstone with low matrix porosity but significant fracture pore space. Note the vertical (bed-normal) stylolite (between red arrows). (8904.5 ft., porosity = 1.4%, permeability = 0.01 mD).

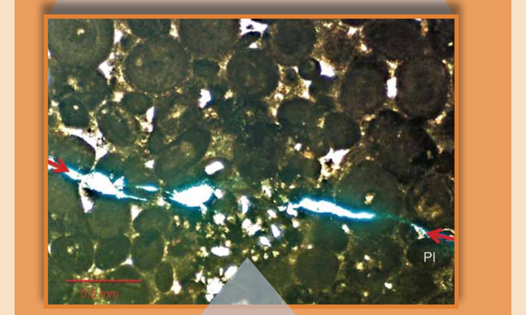

Tight silty oolitic grainstone that displays solution-enlarged subhorizontal microfractures (in blue between the red arrows).

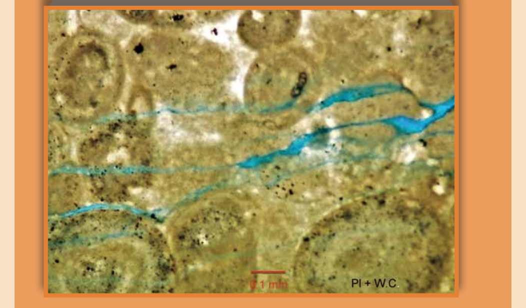

Swarm of solution-enlarged sub-horizontal microfractures cutting across ooids and cements.

Quartz-rich siltstone to fine-grained sandstone displaying pin-stripe lamination and some low-angle cross stratification. Note the small white replacement anhydrite (An) nodules (see red arrows). (8910.5 ft., porosity = 2.4%, permeability = 0.01 mD).

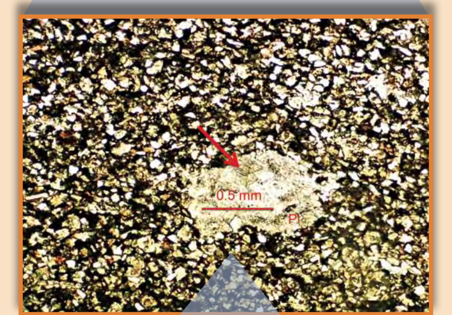

Well-cemented calcareous siltstone with a replacement anhydrite nodule (see red arrow).

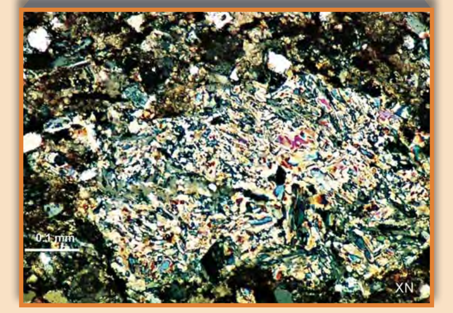

Highly magnified view of an anhydrite replacement nodule.

Quartz-rich siltstone to fine-grained sandstone exhibiting low-angle cross stratification and abundant white anhydrite (An) nodules. (8913.5-14 ft., porosity = 3.3%, permeability = 0.01 mD).

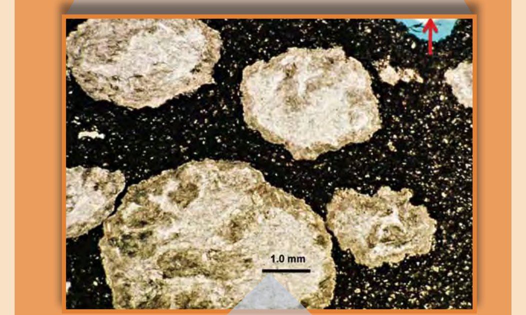

Cluster of small replacement anhydrite nodules within a very low porosity siltstone.

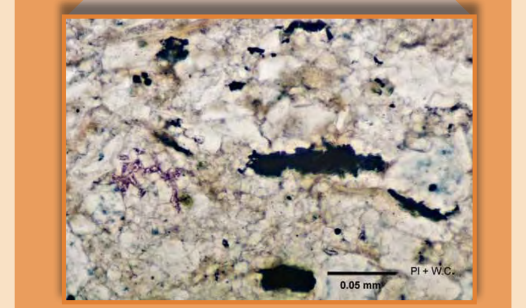

Highly magnified view of very well-cemented quartz siltstone. Note the abundant amount of opaque sulfide minerals as well as ferroan calcite (stained purple) and ferroan dolomite (stained blue) cements.

Rich Member

Core Description

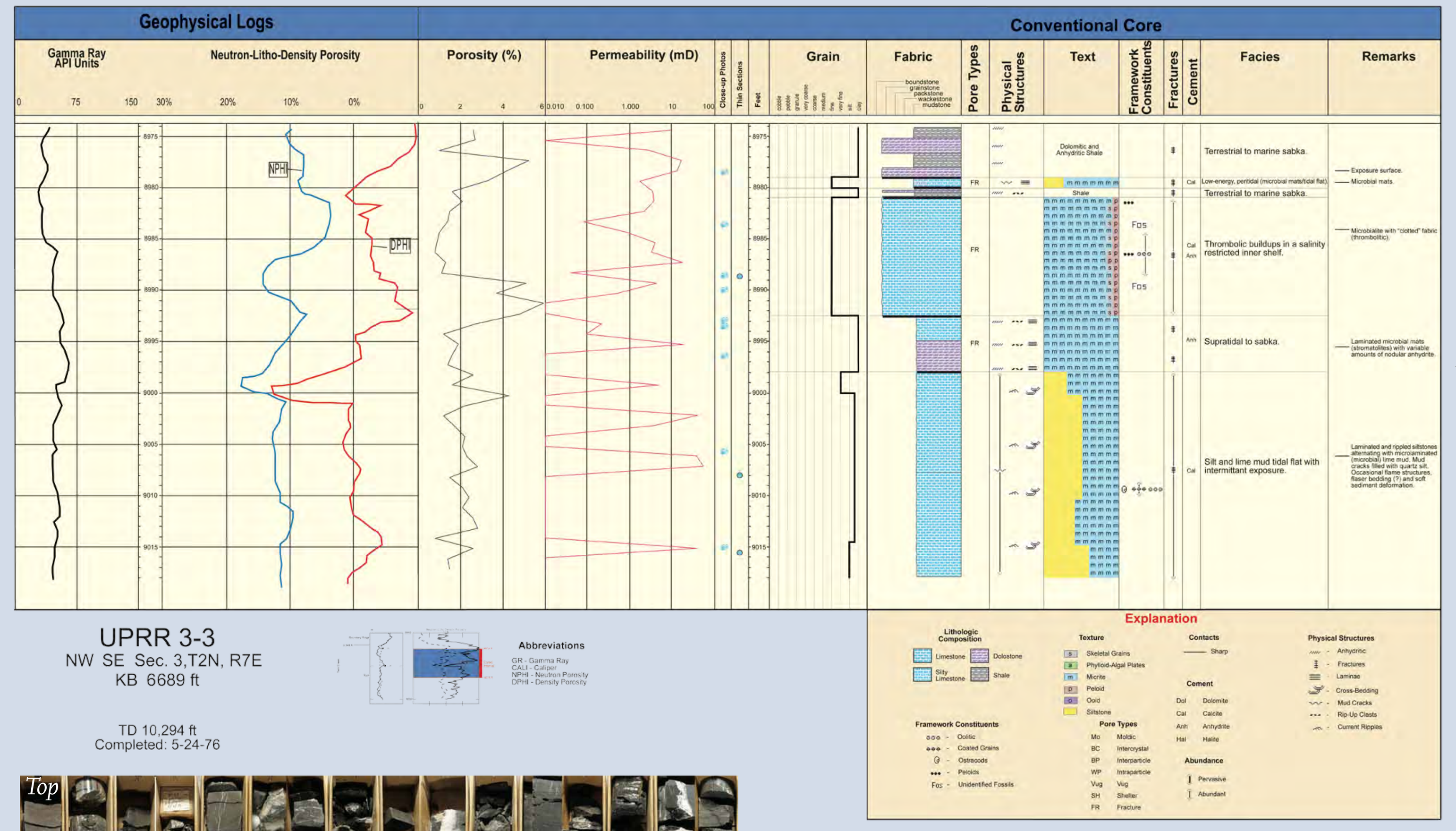

Core through the Rich Member: 8974 – 9018 ft.

Porosity/Permeability Cross Plot

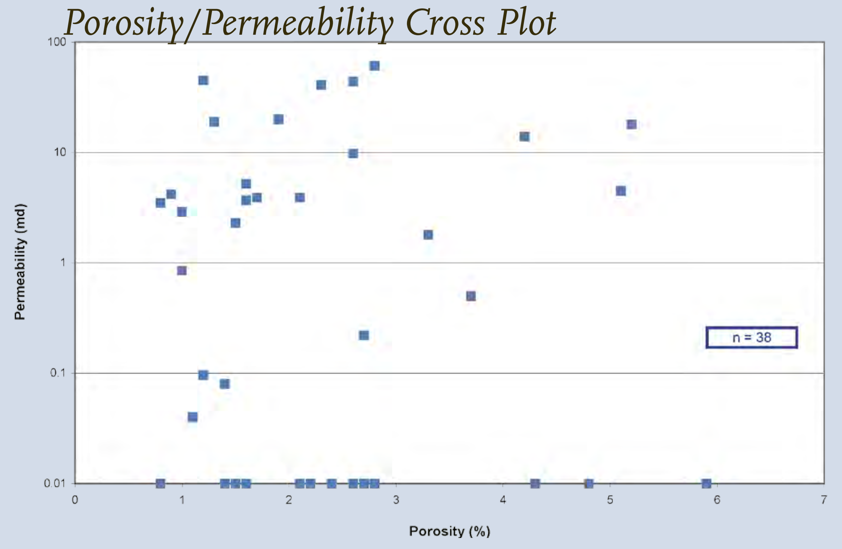

Exposure surface marked by dolomitic mud rip-up intraclasts derived from desiccation cracked surfaces. Note the mineralized vertical fractures (in white). (8978.5 ft., porosity = 4.2%, permeability = 14 mD).

Microbial boundstone/oolitic grainstone displaying a clotted thrombolitic fabric. Anhydrite has filled space between possible solution-collapse breccia and fractures. (8983.5 ft., porosity = 1.4%, permeability = 0.08 mD).

Oolitic grainstone in which the individual ooids (in dark gray) are highly deformed by burial-related pressure solution. There is no visible matrix porosity. Note the significant patches of replacement anhydrite (An) as well as the fracture swarms healed with anhydrite (in white). There may be minor open segments along some microfractures (see red arrows). (8988.7 ft., porosity = 1.4%, permeability = 0.04 mD).

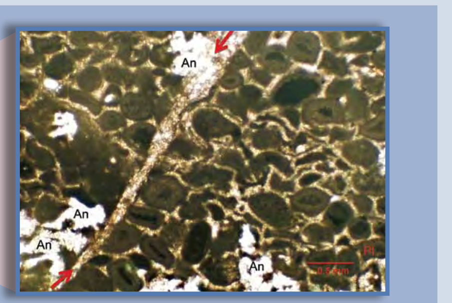

Deformed ooids and flattened isopachous cements due to pressure-solution processes. Note the calcite-filled tension gash (between red arrows) as well as small patches of replacement anhydrite (An).

Microbial boundstone that displays a thrombolitic texture. Note the mineralized vertical and oblique fractures (in white). (8990 ft., porosity = 5.1%, permeability = 4.5 mD).

Nodular to "chicken-wire" anhydrite (in white) that grew displacively within a limy to dolomitic mudstone. (8993 ft., porosity = 4.8%, permeability = 0.01 mD).

Microbial mudstone displaying a laminated stromatolite structures. Note the displacive and replacive white anhydrite nodules as well as vertical fractures healed with anhydrite. (8993.6 ft., porosity = 2.7%, permeability = 0.22 mD).

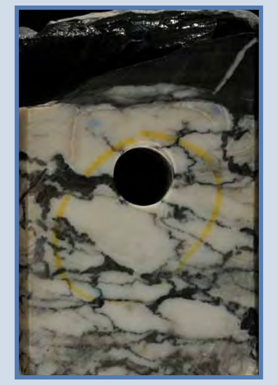

White anhydrite displaying coalesced nodular to "chicken-wire" fabric within a dolomitic mudstone host. (8996.4 ft., porosity = 1.6%, permeability = 0.01 mD).

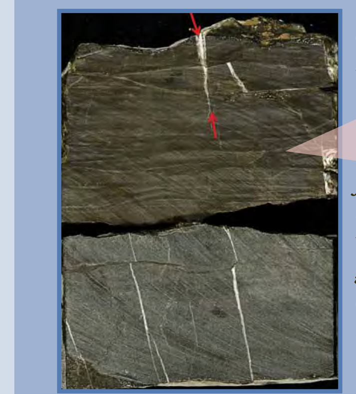

Oolitic grainstone bound and laminated by microbial structures. The ooids within this interval display syndepositional breakage and "cerebroid" margins. These ooids probably formed within a hypersaline lagoon. Note the two types of vertical fractures: (1) a tensional gash (between the red arrows), and (2) vertical tectonic fractures healed with white calcite. (9008 ft., porosity = 1.5%, permeability = 0.01 mD).

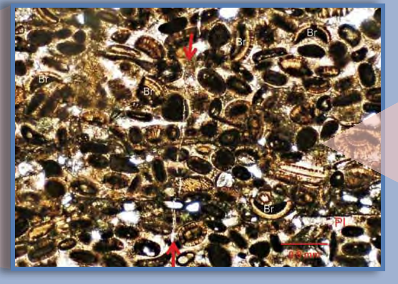

Oolitic/skeletal grainstone diluted with quartz silt grains. Note the abundance of broken ooids (Br) as well as the complex cementation that occluded all matrix pores. A microfracture (between red arrows) is healed with calcite.

View of ooids, skeletal grains, peloids and quartz grains completely surrounded by calcite cements (stained pink). Note the broken ooids (Br), which are probably indicative of formation under elevated salinity. For instance, broken ooids are common in modern Great Salt Lake hypersaline carbonate sediments.

Close-up view of a syndepositionally deformed ooid with scalloped margins (see red arrows). This is a "cerebroid ooid" and is a common form within hypersaline environments like the modern Great Salt Lake.

Close-up view of some syndepositionally deformed ooids that have been healed with regenerated oolitic coatings. Note the cerebroid ooids (with red arrows showing scalloped margins) and the broken ooid (Br + Re). These two types of ooids are the result of radial internal fabrics, which typically form in hypersaline settings.

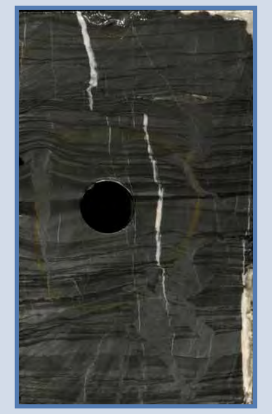

Alternating thin beds of quartz-rich siltstone and lime mudstone that have been disrupted by silt-filled desiccation cracks. Note the vertical fractures that have been healed with white anhydrite. (9005.6 ft., porosity = 2.1%, permeability = 0.01 mD).

Close-up view of thin-bedded and laminated calcareous siltstone that has been disrupted by compacted, silt-filled desiccation cracks. Note the vertical fractures filled with white anhydrite. (9015 ft., porosity = 0.8%, permeability = 0.01 mD).

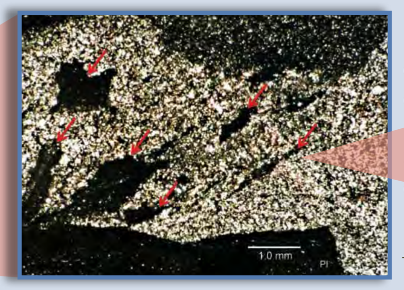

Tight siltstone with calcite cements. Note the angular rip-up clasts (see red arrows) that may be the result of desiccation and subaerial exposure. (9015.5 ft., porosity = 2.6%, permeability = 44 mD).

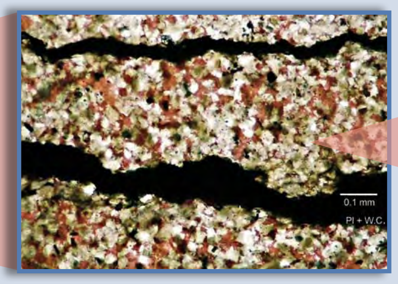

Tight quartz- and carbonate grain-rich siltstone with calcite cements (stained red). Black (opaque) insoluble residues mark stylolites that cut across this siltstone.

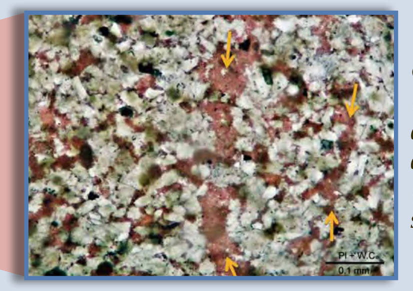

Calcite-filled microfractures (between yellow arrows) as well as calcite-cemented quartz-rich siltstone. (Calcite has been artificially stained red).

Lithofacies and Petrography

Sliderock Member

Core Description

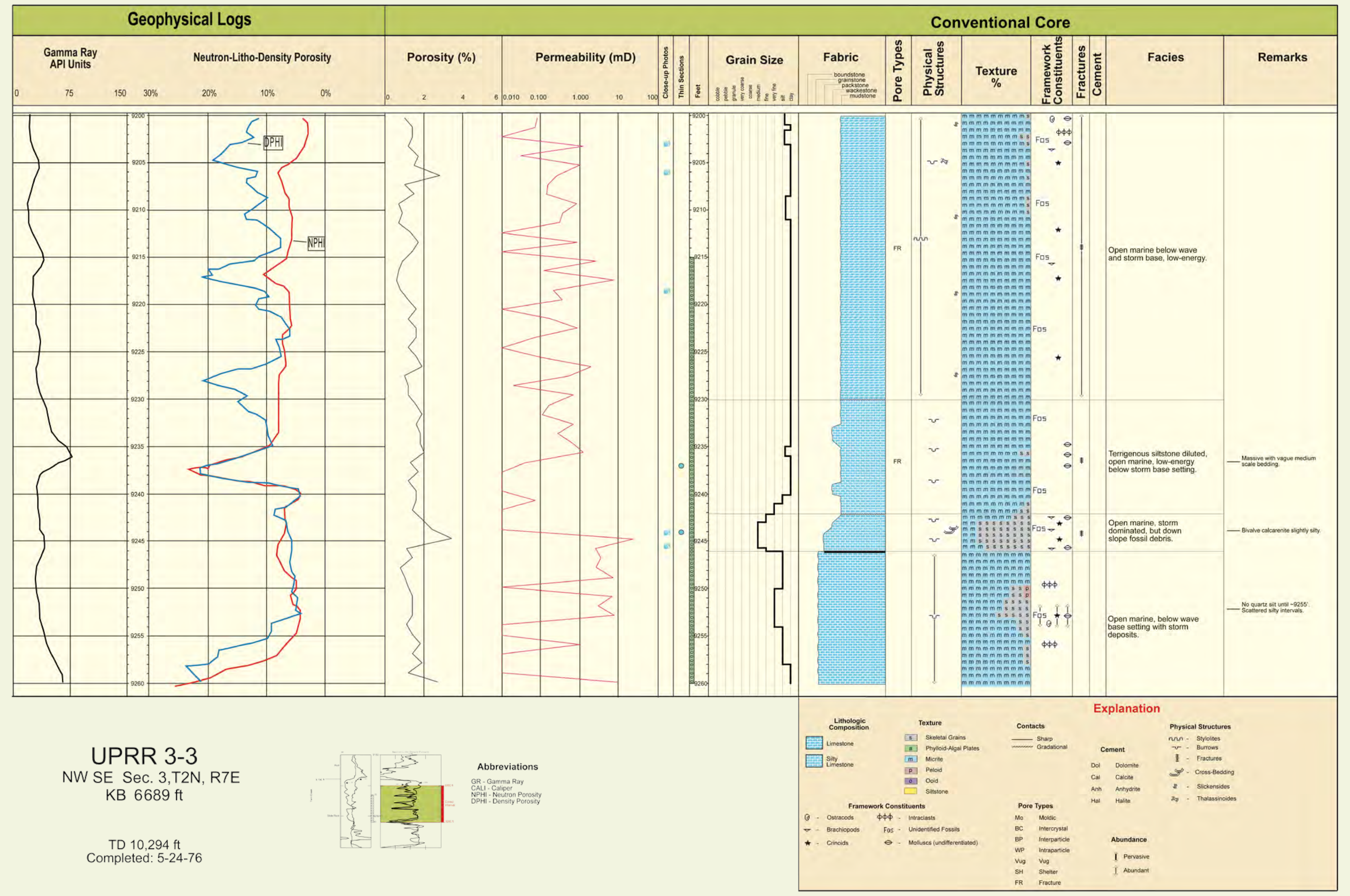

Core through the Sliderock Member: 9200 – 9260 ft.

Crinoidal wackestone that displays bioturbation and small desiccation cracks. The white specks are mostly crinoids. Possible open fractures are noted by red arrows within this perforated interval. (9203 ft., porosity = 1.3%, permeability = 1.2 mD).

Mineralized fracture surface from perforated zone. The red arrows show some of the stair step-type surfaces on the calcite fracture lining. Note the light brown oil staining. (9206 ft., porosity = 2.9%, permeability = 0.26 mD).

Lime mudstone with a swarm of vertical (bed-normal) stylolites (see red arrows) and mineralized fractures (in white). Some of the calcite-filled fractures cross cut and postdate the vertical stylolites. (9218.8 ft., porosity = 0.9%, permeability = 0.21 mD).

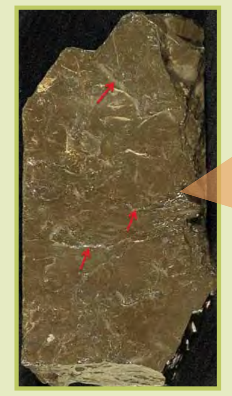

Natural vertical fracture surface in a massive silty lime mudstone. The red arrows point to lightly mineralized, multiple stair-step surfaces that indicate an open fracture through this core interval. (9237 ft., porosity = 1.8%, permeability = 0.01 mD).

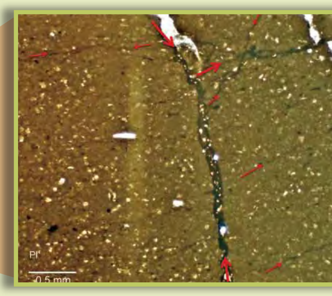

Low porosity silty peloidal mudstone to peloidal/skeletal wackestone that displays possible open microfractures (see red arrows). Some of the microfractures may have followed earlier stylolites of both horizontal and vertical orientations. Both insoluble residues and oil staining give these "stylo-fractures" their dark color in thin section. Later "tension gash" fractures have been healed with calcite (in white).

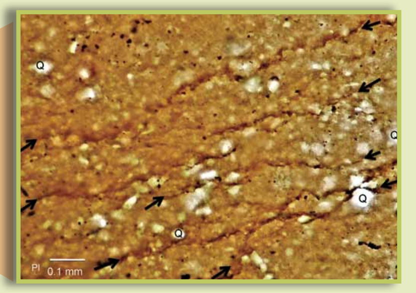

High magnification view of a very low porosity silty lime mudstone matrix exhibiting a network of stained microfractures (between black arrows) that probably originated as wispy microstylolites. Detrital quartz grains (Q) are scattered through the mudstone matrix.

Porosity/Permeability Cross Plot

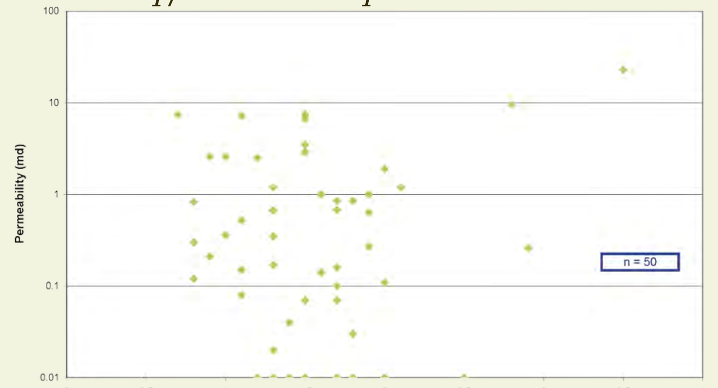

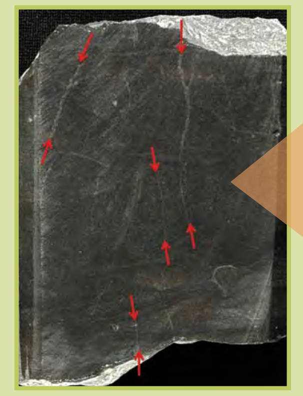

Bedded skeletal/peloidal packstone to grainstone with several sub-vertical microfractures (between red arrows) that appear to be open. This core segment is from a perforated interval. (9244 ft., porosity = 3.5%, permeability = 23 mD).

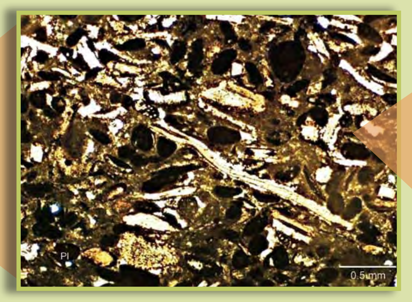

Skeletal/peloidal grainstone to packstone. Note the absence of any visible matrix porosity within this calcarenite.

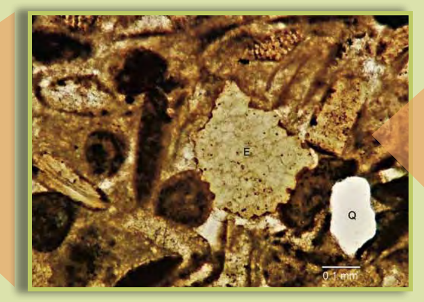

Close-up view of various skeletal fragments, hard peloids and coated grains within this well-sorted grainstone/packstone. Note the echinodern plate (E) and the detrital quartz grain (Q) that show pressure-solution contacts without carbonate grains.

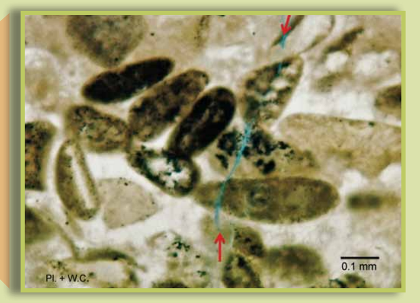

View of an open microfracture (impregnated with blue-dyed epoxy between the red arrows) that cuts across carbonate grains and cements.

Bedded skeletal/peloidal packstone/grainstone alternating with lime mudstone/wackestone. Note the probable open microfracture between the red arrows. (9245.5 ft., porosity = 1.2%, permeability = 2.5 mD).

Outcrop Analogs

Devils Slide, Weber Canyon, Utah

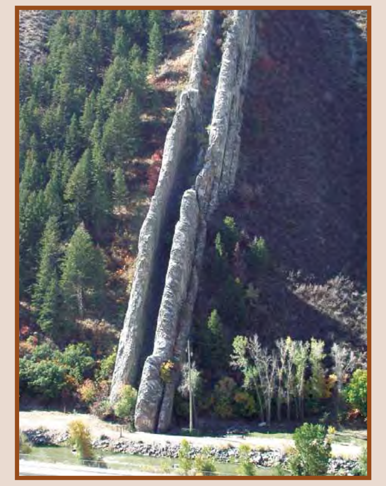

This famous landmark is composed of resistant and non-resistant units of the Boundary Ridge Member of the Twin Creek Limestone. The Boundary Ridge consists of mostly red and green-gray mudstone and calcareous siltstone with thin, interbedded, dense limestone. The Devils Slide is two of the resistant limestone units separated by a non-resistant red-brown calcareous siltstone.

Geologic Map of the Devils Slide Area, Morgan and Summit Counties, Utah

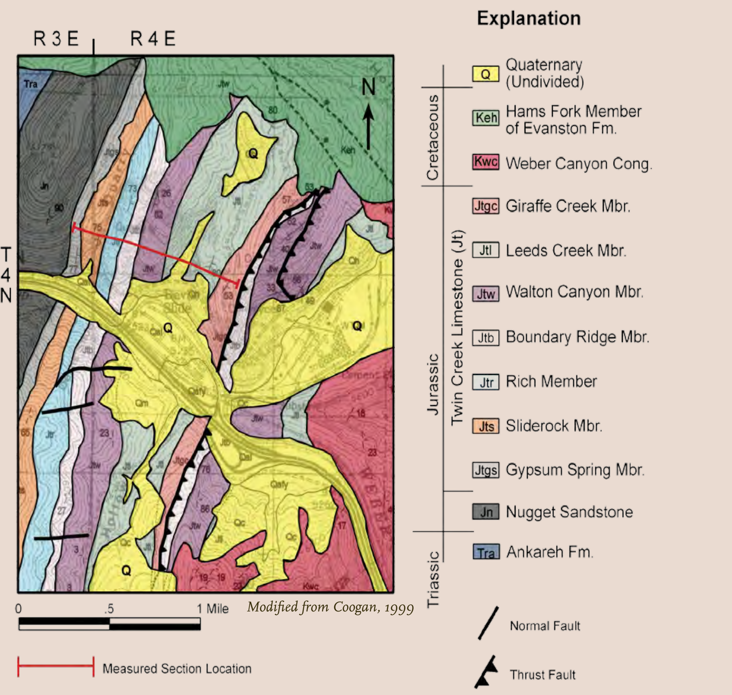

Geologic Map of the Peoa Area, Summit County, Utah

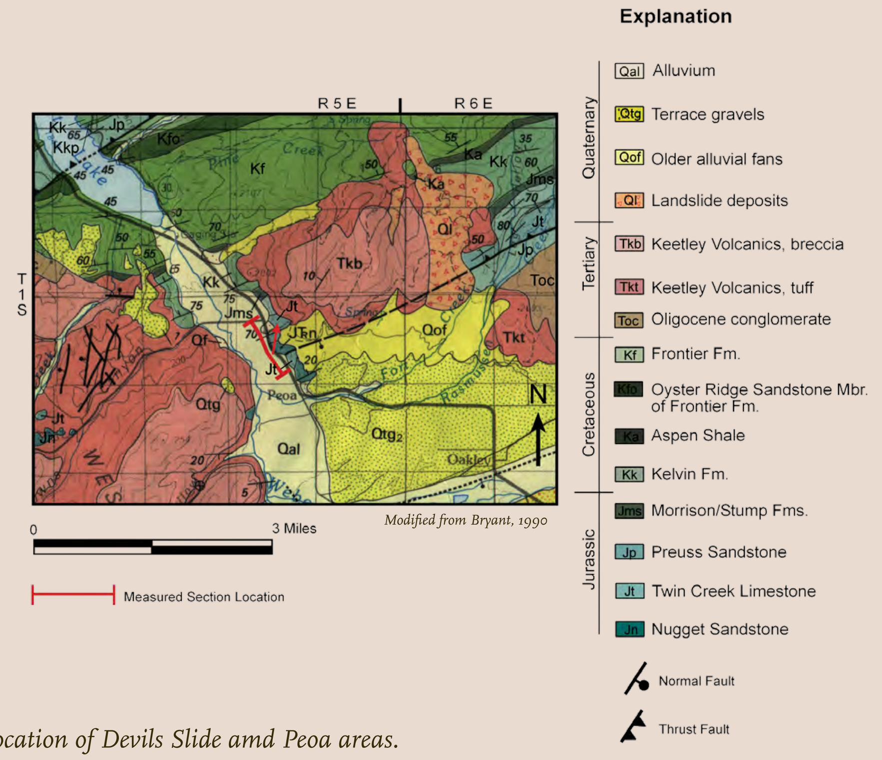

See Twin Creek oil and gas fields map on panel 1 for location of Devils Slide amd Peoa areas.

Characteristics of the Watton Canyon Member of the Twin Creek Limestone

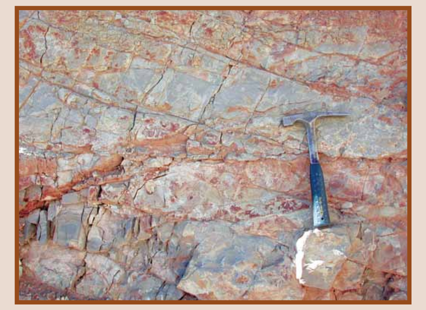

Closely spaced rectilinear fracturing in dense, micritic limestone, Devils Slide section.

Large-scale, well-displayed rectilinear fracturing in steeply dipping limestone, Devils Slide section.

Large-scale, open fractures on bedding plane surface, Devils Slide section.

Well-displayed rectilinear fracturing on top of the Watton Canyon Member, Peoa section.

Contact between fractured Watton Canyon Member limestone and basal argillaceous unit of the overlying Leeds Creek Member, Peoa section.

Heterogeneity within the Watton Canyon Member caused by thin-bedded siltstone, Devils Slide section.

Characteristics of the Rich Member of the Twin Creek Limestone

Well-developed current ripples on bedding surface with silt-filled fractures, Devils Slide section.

Rhombic fracture patterns on bedding planes, Devils Slide section.

Rhombic fracture patterns on bedding planes, Peoa section.

Closely spaced rectilinear fracturing, Peoa section.

Pencil weathering, Peoa section.

Contact between fractured Rich Member limestone and basal siltstone of the overlying Boundary Ridge Member, Peoa section.

Conclusion & Summaries

- Traps in the Twin Creek Limestone form on discrete subsidiary closures along major ramp anticlines where the low-porosity carbonates are extensively fractured. The seals for the producing horizons are overlying argillaceous and clastic beds, and non-fractured units within the Twin Creek.
- Most oil and gas production is from perforated intervals in the Watton Canyon and Rich Members of the Twin Creek Limestone. These members have little to no matrix porosity in the producing horizons, but exhibit secondary porosity in the form of fractures. Identification and correlation of barriers and baffles to fluid flow, and recognizing fracture set orientations in individual Twin Creek reservoirs in the thrust belt is critical to understanding their effects on production rates, petroleum movement pathways, and horizontal well plans.
- Analysis of core from Pineview field in the northern Utah part of the thrust belt revealed complex reservoir heterogeneity due to a variety of carbonate lithofacies, textures, structures, and diagenesis (fracturing and stylolitization). Lithofacies include open marine, low- to high-energy middle shelf, microbial tidal flat, marine sabkha, inner shelf microbial lagoon, oolitic shoals, and terrestrial siliciclastics. Carbonate fabrics consist of microbially laminated mudstone, wackestone, packstone, grainstone/rudstone, and thrombolite boundstone with beds of siltstone and shale.
- Oil-productive fractures display a complex history of opening, calcite filling, and dissolution. Visible porosity occurs as isolated dissolution pores and partially open microfractures. Replacement dolomite, microporosity, pyrite, and late calcite were controlled by fractures or stylolites.
- The best outcrop analogs for the Twin Creek Limestone reservoir are found west of Pineview field at Devils Slide on the Crawford thrust plate and southwest of Pineview field near the town of Peoa, Utah, on the Absaroka thrust plate(?). Closely spaced rhombic and rectilinear fracture patterns developed on bedding planes and within dense, homogeneous non-porous (in terms of matrix porosity) limestone beds of the Watton Canyon and Rich Members. The contact with the basal siltstone units (where fractures are sealed) of the overlying members set up the Watton Canyon and Rich Members for hydrocarbon trapping and production. Thin-bedded siltstones within the Watton Canyon and Rich Members, also observed in outcrop, create additional reservoir heterogeneity. The outcrop analogs are particularly valuable in examining the interplay of various Twin Creek lithologies and fracture development.

Acknowledgments

Funding for this research was provided, in part, under the Preferred Upstream Management Program of the U.S. Department of Energy, National Energy Technology Laboratory, Tulsa, Oklahoma, contract number DE-FC26-02NT15133. Support was also provided by the Utah Geological Survey (UGS) and Eby Petrography & Consulting, Inc.

The poster design was by Stevie Emerson of the UGS. Cheryl Gustin, James Parker (deceased), and Sharon Wakefield (retired) of the UGS prepared the figures; Michael D. Laine, Thomas Dempster, and Brad Wolverton of the UGS Core Research Center prepared and photographed the cores.

References

Bryant, B., 1990, Geologic map of the Salt Lake City 30' x 60' quadrangle, north-central Utah, and Uinta County, Wyoming: U.S. Geological Survey Miscellaneous Investigation Series Map I-1944, 1:100,000.

Coogan, J.C., 1999, Progress report geologic map of the Devils Slide quadrangle, Morgan and Summit Counties, Utah: unpublished 1:24,000 map used to compile the Ogden 30' x 60' quadrangle, Utah Geological Survey Open-file Report 380, 1:100,000.

Gibson, R.I., 1987, Basement tectonic controls on structural style of the Laramide thrust belt interpreted from gravity and magnetic data, *in* Miller, W.R., editor, The thrust belt revisited: Wyoming Geological Association 38th Field Conference Guidebook, p. 27-35.

Hintze, L.F., and Kowallis, B.J., 2009, Geologic history of Utah: Brigham Young University Geology Studies Special Publication 9, 225 p.

Kocurek, G., and Dott, R.H., Jr., 1983, Jurassic paleogeography and paleoclimate of the central and southern Rocky Mountains region, *in* Reynolds, M.W., and Dolly, E.D., editors, Symposium on Mesozoic paleogeography of west-central U.S.: Society for Sedimentary Geology (SEPM), Rocky Mountain Section, p. 101-116.

Sprinkel, D.A., and Chidsey, T.C., Jr., 1993, Jurassic Twin Creek Limestone, *in* Hjellming, C.A., editor, Atlas of major Rocky Mountain gas reservoirs: New Mexico Bureau of Mines and Mineral Resources, p. 76.

Utah Division of Oil, Gas, and Mining, 1997a, Structure map of top Watton Canyon, Pineview field: Cause No. 167-8, Exhibit No. P-5, 1 inch = 4000 feet.

Utah Division of Oil, Gas, and Mining, 1997b, Structural cross section, Pineview field: Cause No. 167-8, Exhibit No. P-6.

Reservoir and Production Data Sources

Cook, C.W., and Dunleavy, J.R., 1996, Pineview, *in* Hill, B.G., and Bereskin, S.R., editors, Oil and gas fields of Utah: Utah Geological Association Publication 22 (Addendum), non-paginated.

Moore, B.J., and Sigler, S., 1987, Analyses of natural gases, 1917-1985: U.S. Bureau of Mines, Information Circular 9129, 1197 p.

Utah Division of Oil, Gas, and Mining, 2009, Oil and gas production report, November: Online, https://fs.ogm.utah.gov/pub/oil&gas/Publications/Reports/Prod/Well/Wel_Nov_2009.pdf., accessed March 4, 2010.

Utah Division of Oil, Gas, and Mining, well completion files.

Dislcaimer